

Article

Occurrence Characteristic and Mining Technology of Ultra-thick Coal Seam in Xinjiang, China

Dongdong Qin ¹, Xufeng Wang ^{1,2,3,*}, Dongsheng Zhang ^{1,3}, Weiming Guan ^{1,4}, Lei Zhang ¹ and Mengtang Xu ⁵

¹ School of Mines, China University of Mining & Technology, Xuzhou 221116, China; qindongdong@cumt.edu.cn (D.Q.); zhangds@cumt.edu.cn (D.Z.); gwmxju@xju.edu.cn (W.G.); Lei-zhang@cumt.edu.cn (L.Z.)

² Jiangsu Engineering Laboratory of Mine Earthquake Monitoring and Prevention, China University of Mining & Technology, Xuzhou 221116, China

³ State Key Laboratory of Coal Resources and Safe Mining, China University of Mining & Technology, Xuzhou 221116, China

⁴ College of Geology and Mining Engineering, Xinjiang University, Urumqi 830046, China

⁵ School of Mines, Guizhou Institute of Technology, Guiyang 550003, China; xumtcumt@cumt.edu.cn

* Correspondence: wangxufeng@cumt.edu.cn

Received: 6 October 2019; Accepted: 13 November 2019; Published: 17 November 2019



Abstract: The scientific and efficient mining of ultra-thick coal seam in Xinjiang, China is faced with the problems of low exploration level and lack of theoretical research on underground mining. This paper studied occurrence characteristic of ultra-thick coal seams in Xinjiang, using field investigation and drilling exploration. Based on the variation law of support load under different roof bearing structure form and development height in multi-layer mining, classification method and mining technology selection of ultra-thick coal seam were put forward. The results indicate that: (1) The ultra-thick coal seams in Xinjiang have a distribution characteristic of more north and less south, more east and less west, mainly concentrate in East Junggar and Turpan-Harmi coalfields. The form of the ultra-thick coal seam has the remarkable characteristic of coal seams merging and bifurcating. (2) The mechanical model of the relationship between the support and surrounding rock under different roof bearing structures is established. At the early stage of multi-layer mining, the support load includes the load caused by rotary subsidence of the blocks that formed the near-stope roof bearing structure and the gravity load of rock blocks under roof bearing structure. At the later stage, the support load is mainly gravity load of loose blocks below the far-stope roof bearing structure. (3) According the roof bearing structure form, ultra-thick coal seam can be divided into three types: no stable bearing structure, (higher) beam bearing structure and arch bearing structure. In order to ensure the stability of near-stope roof bearing structure, backfill mining, longwall mining, and longwall mining early and backfill mining later should be adopted in three types ultra-thick coal seams mining respectively.

Keywords: ultra-thick coal seam; shield and surrounding rock interaction; roof bearing structure; mining technology; multi-layer mining

1. Introduction

Occurrence of ultra-thick coal seam is a common phenomenon. Coalfields with single seam thickness of more than 20 m distribute in major coal-mining countries and regions such as China, United States, Russia, Eastern Europe and Southeast Asia. The integrated coalfield with ultra-thick coal seam has the characteristics of good production conditions, low mining cost and large output. In order to mine ultra-thick coal seams scientifically, researchers have studied occurrence and genesis of the ultra-thick coal seams [1,2].

In terms of occurrence characteristics of ultra-thick coal seams, the Carboniferous ultra-thick coal seams occur from Europe to Central Asia [3], the Permian ultra-thick coal seams distribute in Gondwana [4–7], which is composed of Australia and India, and the Carboniferous-Permian ultra-thick coal seams are mainly bituminous coal with concentrated occurrence and high metamorphic degree; the Jurassic ultra-thick coal seams distribute along latitudes in Kazakhstan, Russia, Xinjiang and Ordos Basin in China, mainly with non-caking coal and lignite [8]; tertiary ultra-thick coal seams widely distribute around the world, but the degree of coal metamorphism is low, mainly lignite.

Traditionally, it is considered that the thick coal seam is the product of long-term equilibrium compensation between peat accumulation rate and basement subsidence rate, but it is difficult to explain the process mechanism of continuous peat deposition forming ultra-thick coal seam [9–11]. Relevant experts and scholars have studied the genesis mechanism of ultra-thick coal seam based on different examples. Diessel et al. [12,13] proposed the transgressive regressive sequence model of coal seam sediments, identified and divided the sequence boundary of ultra-thick coal seam, which laid a foundation for studying the genesis mechanism of ultra-thick coal seam with regional distribution. Wu et al. [14] studied genesis of ultra-thick coal seam in typical fault basins, and believed that the allochthonous accumulation of peat caused by storms, gravity flow and underwater debris flow played a very important role in the development of ultra-thick coal seam. They established the genetic model of allochthonous accumulation in deep water environment of ultra-thick coal seam. Shearer thought that thick coal seam is composed of several ancient peat bodies, which are separated by the interface that marks the falling water level. Based on this, Banerjee et al. [15] believed that ultra-thick coal seam may be a complex of multiple high-frequency sequences in the interior. On the basis of previous studies [16], Wang et al. [2,17] put forward genetic model of ultra-thick coal seams formed by superimposition of multiple coal seams. They believed that the formation of ultra-thick coal seams in the depression basin was the result of superposition of multiple coal seams.

There are ultra-thick coal seams in Xinjiang, Liaoning, Inner Mongolia and Yunnan of China. As well, except Laohutai coal mine in Fushun, which adopts slicing sand backfill mining, open-pit mining is usually adopted in ultra-thick coal seams. As a key coal base of 100 million tons in China, Xinjiang has four major integrated coalfields, being East Junggar, Ili, Turpan-Harmin and Kuqa-Bay coalfields [18]. The presence of ultra-thick coal seams, which are usually more than 20 m thick, is an important feature in East Junggar, Turpan-Harmin and Ili coalfields. For example, in East Junggar Coalfield, a single seam with thickness more than 80 m has been reported, and there is a ultra-thick coal seam in Shaerhu coalfield, with thickness more than 200 m. As the focus of Chinese coal resources development shifted to the western region, the coal output in Xinjiang has increased from 88.12 million tons in 2009 to 167 million tons in 2017, and will be further expanded in the future. However, at present, the area is facing the problems of low exploration level (only 46% of geological resources are identified) and lack of design and practical experience for ultra-thick coal seam underground mining. Most mines are in the planning stage. Based on distribution and occurrence characteristic of ultra-thick coal seam in Xinjiang, this paper theoretically analyses the variation characteristic of the support load under different roof bearing structures, classifies ultra-thick coal seams according to the occurrence conditions, and puts forward the appropriate mining technology. The results will provide a guideline for the mining area construction and coal mining method selection under similar mining conditions.

2. Distribution Characteristic of Ultra-thick Coal Seams in Xinjiang

The distribution of main coalfields in Xinjiang is shown in Figure 1. Coal resources mainly distribute in the north and east, accounting for 94.7% of the total forecast reserves, and there are 24 coalfields with forecast reserves of more than 10 billion tons.

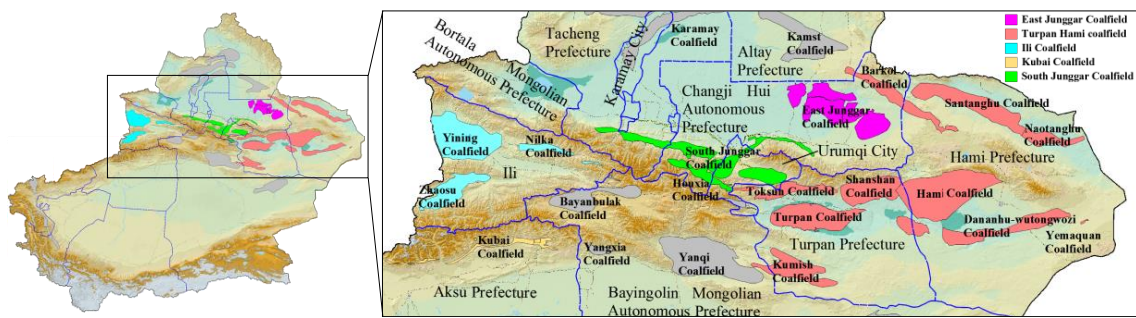


Figure 1. Distribution of main coalfields in Xinjiang.

The coalfields with forecast reserves of more than 100 billion tons are East Junggar coalfield, Shaerhu coalfield, Yining coalfield, Turpan coalfield and Dananhu-Wutongwozi coalfield, accounting for about 60% of the total forecast. According to the distribution and development strategy of coal resources in Xinjiang, four major coalfields, East Junggar, Ili, Turpan-Harmi and Kuqa-Bay Coalfields, are planned to be the main bases of Xinjiang coal power, “coal transportation from west to east” and coal-to-gas.

The distribution of the ultra-thick coal seams in Xinjiang is shown in Figure 2. There are ultra-thick coal seams in the three integrated coalfields of East Junggar, Turpan-Harmi and Ili. Reserves of ultra-thick seams and planned coal production in each coalfields are shown in Figures 3 and 4.

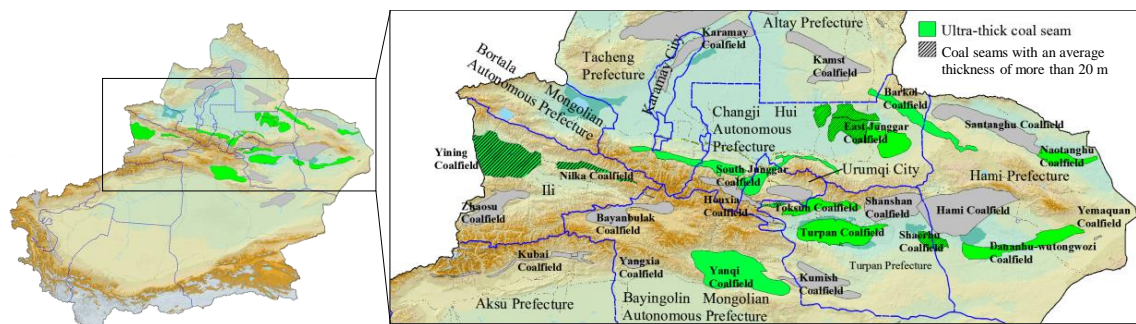


Figure 2. Distribution of ultra-thick coal seams in Xinjiang.

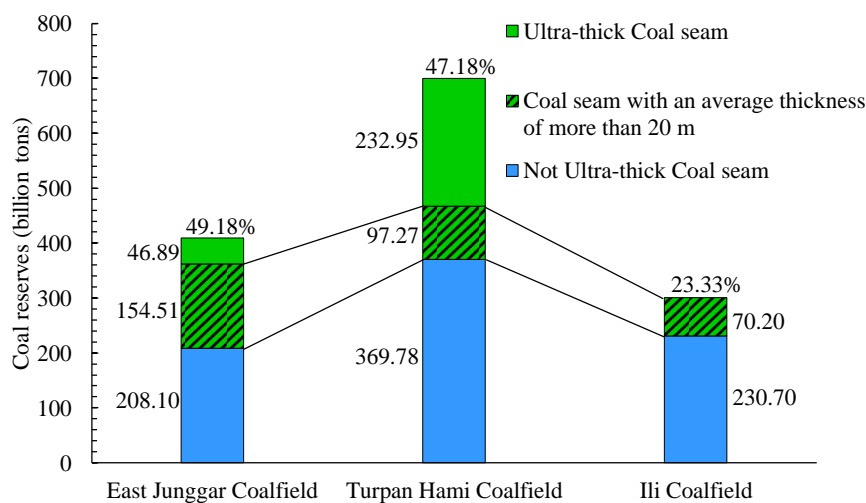


Figure 3. Reserves of ultra-thick coal seams in three coalfields.

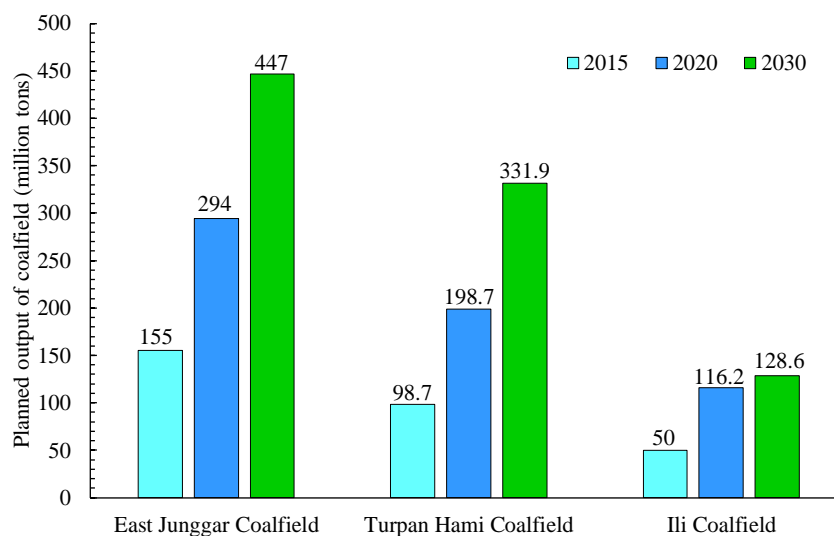


Figure 4. Planned coal production in three coalfields.

The distribution of ultra-thick coal seams in Xinjiang is characterized by more north and less south, and more east and less west, and coal seams mainly concentrate in East Junggar and Turpan-Harmi coalfields. The proven reserves of ultra-thick coal seams in the East Junggar, Turpan-Harmi and Ili coalfields account for 27.49% of the total forecast reserves in Xinjiang. As well, the reserves of ultra-thick coal seams in the three coalfields are 201.40 billion tons, 330.23 billion tons and 70.20 billion tons respectively, accounting for 49.18%, 47.18% and 23.33% of the forecast reserves in their respective coalfields. The planned output of East Junggar coalfield will increase from 155 million tons in 2015 to 447 million tons in 2030, an increase of 1.88 times, accounting for 49.26% of the planned output of the three integrated coalfields. It is the key development coalfield in Xinjiang coal base. In the construction process of East Junggar coal base, it will inevitably encounter the problem of ultra-thick seam underground mining.

3. Occurrence Characteristic of Typical Ultra-thick Coal Seams

Most ultra-thick coal seams distribute in East Junggar and Turpan-Harmi coalfield in the eastern part of Xinjiang. As well, ultra-thick coal seams with average thickness of more than 20 m are concentrated in Shaerhu coalfield and East Junggar coalfield. Therefore, taking these two typical coalfields as examples, this paper analyses occurrence characteristic of ultra-thick coal seams in Xinjiang.

3.1. Occurrence of Shaerhu Coalfield

The main structural unit of Shaerhu coalfield is Shaerhu depression in the southern depression zone, adjacent to Toksun depression and Shaerhu uplift in the north, Aydingkol slope in the west, and Wutongwozi depression in the east, as shown in Figure 5 [19]. Figure 6 shows contour distribution of coal seam thickness and section of eastern coal seam in Shaerhu coalfield.

The coal seam in Shaerhu coalfield is located in the middle section of middle Jurassic Xishanyao formation (J_2x). It can be divided into 25 coal seams, and 23 coal seams can be mined. The C_8 coal seam is main mining seam with a total thickness of 1.30–267.42 m and average thickness of 96.82 m. The coal seam shows bifurcation in the southern part of coalfield, the roof is mudstone and carbonaceous mudstone, while the floor is siltstone and silty mudstone. Mudstone and carbonaceous mudstone are main lithology of roof and floor in the rest of the coalfield. The coal seam is thick in the north, thin in the south, and is deep in the north and shallow in the south. Coal seam depth is mostly within 600 m.

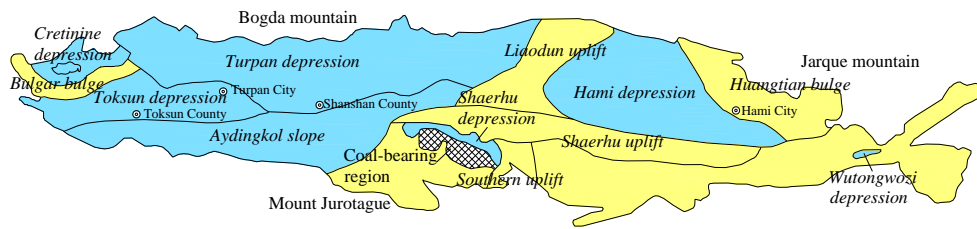
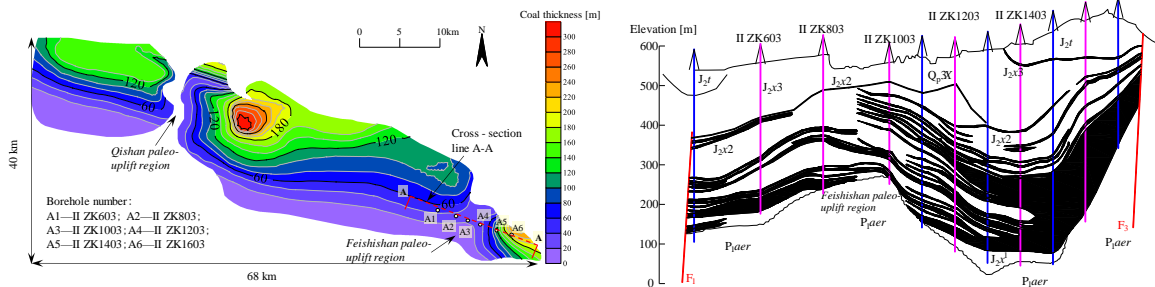


Figure 5. Shaerhu coalfield and its surrounding structural distribution.



(a) Coal seam thickness distribution in shaerhu coalfield

(b) Section A-A of eastern coal seam

Figure 6. Contour distribution of coal seam thickness and section of eastern coal seam in the Shaerhu coalfield.

3.2. Occurrence of East Junggar Coalfield

The main structural unit of the East Junggar coalfield is eastern uplift of Junggar basin, with Kelameili mountain in the north, Bogda mountain in the south, and Donghaidaozi depression, Baijialhai uplift and Fukang depression from north to south in the west. East Junggar coalfield mainly has Wucaiwan, Dajing, Jiangjunmiao, Xiheishan and Laojunmiao mining areas, which are concentrated in the northern part of the coalfield with the boundary of Shaqi uplift, as shown in Figure 7 [20,21].

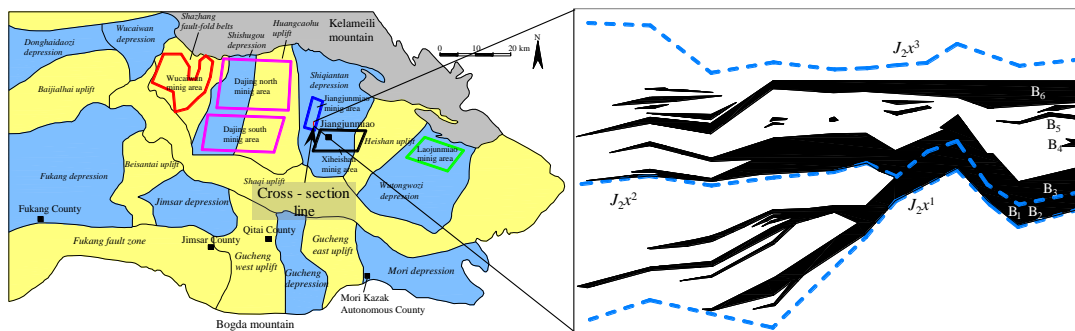


Figure 7. Structure of East Junggar coalfield and section of coal seam.

The major coal-bearing strata in East Junggar coalfield are lower Jurassic Badaowan (J_1b) and middle Jurassic Xishanyao (J_2x) formations. Badaowan formation (J_1b) contains group A coal with a formation thickness of 6.60–120.24 m. The formation thickness decreases from west to east along the strike, and increases from periphery to center of the basin along the trend. The lithology is mainly argillaceous siltstone, silty mudstone, fine sandstone and mudstone. The depression in front of the Bogda mountain contains 5–8 coal seams with a cumulative thickness of 26.65 m, while the depression in front of the Kelameili mountain contains 1–4 coal seams with a cumulative thickness of 7 m. Xishanyao formation (J_2x) contains group B coal, which is the most important coal-bearing formation in East Junggar coalfield. The formation thickness is 18–285 m, and the coal accumulation is the best when the formation thickness is 100–130 m. Dajing mining area is the coal-rich center of group

B coal. The number of coal seams in group B coal increases from east to west, and single coal seam becomes thinner. The thickness of single coal seam in Dajing mining area is up to 70–90 m. The roof and floor of coal seam are mainly fine sandstone, medium sandstone and carbonaceous mudstone, and the burial depth is 300–600 m.

Due to severe deformation of strata in the coal-bearing basin in Xinjiang, there is a big difference in the coal seam dip angle. The dip angle of ultra-thick coal seam is 0–54°, and the number and thickness of the coal seams vary greatly.

3.3. Form of Ultra-Thick Coal Seam

The study area is Dajingnan N°. 1 coal mine, which is located at the junction of the Jiangjunmiao mining area and the Dajing mining area in East Junggar coalfield. A total of 124 boreholes are drilled in this area, and the boreholes arrangement is shown in Figure 8.

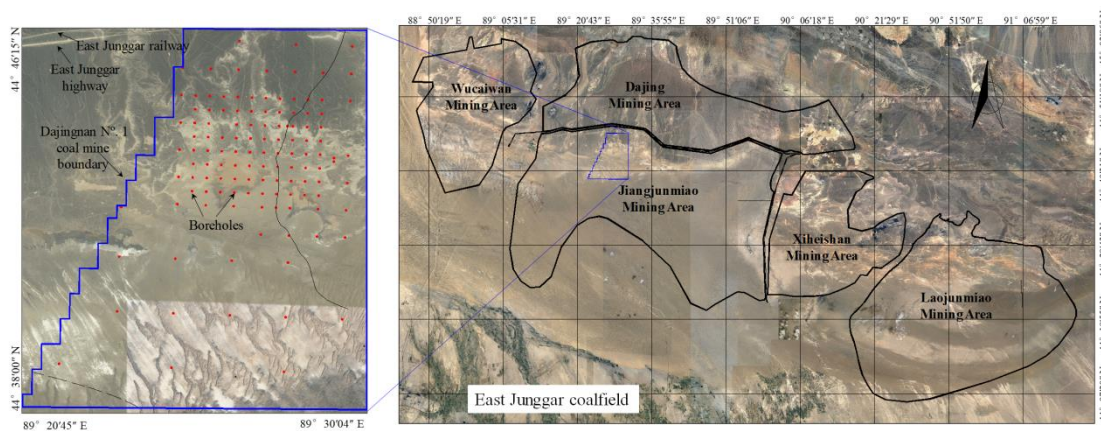


Figure 8. Boreholes arrangement of Dajingnan N°. 1 coal mine.

The form of group B coal in the mine north is obtained by processing the borehole data, as shown in Figure 9a. In order to easy observation, the group B is expanded by 10 times along the thickness direction, the form of group B coal after expanded is shown in Figure 9b.

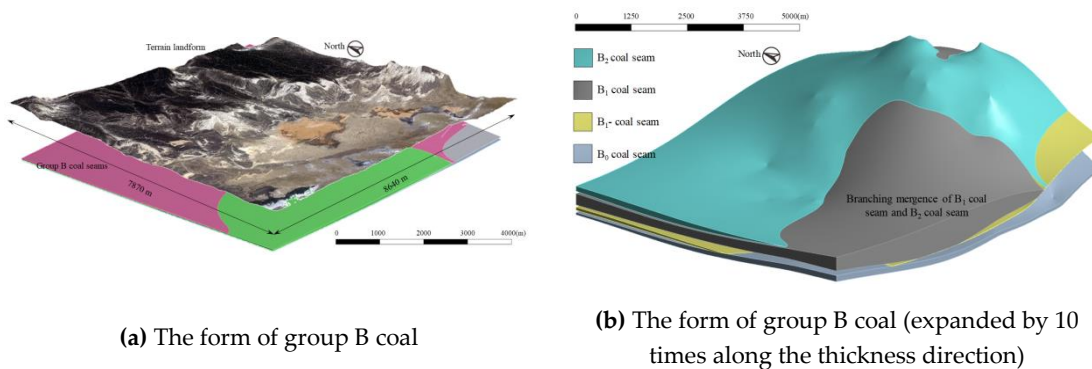


Figure 9. The form of group B coal in the north of Dajingnan N°. 1 coal mine.

The section of group B coal at different positions in the northern region of the mine is shown in Figure 10. The form of group B coal presents the characteristics of the northern coal seams merged and the southern coal seams bifurcated. As well, the thickness of the coal seam in the northwest is large, the thickness in the southeast is relatively small. The distance between the coal seams is 0–40 m.

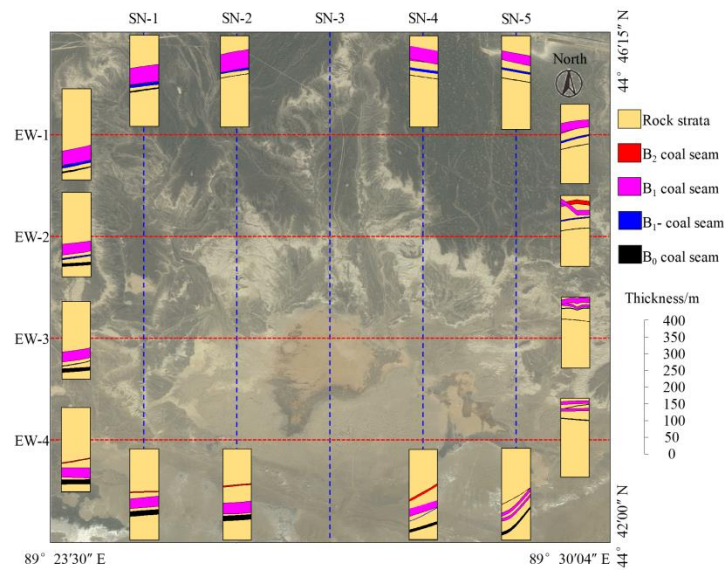


Figure 10. The section of group B coal at different positions in the mine.

It is generally believed that the formation of ultra-thick coal seam has experienced multiple sedimentary discontinuities, and it is an integration of multiple coal seams. Therefore, in the form of the ultra-thick coal seam, it has the remarkable characteristics of coal seams merging and bifurcating. As well, the form of group B in the Dajingnan N^o. 1 coal mine is verified for this.

From the perspective of coal seam form, there are two forms of ultra-thick coal seam: single ultra-thick coal seam and close distance thick coal seam group. Considering the influence of ultra-thick coal seam mining on the roof, the ultra-thick coal seam can be divided into two types: Type A, single ultra-thick coal seam and ultra-close distance thick coal seam group (the comprehensive mining thickness of the upper and lower coal seams is close to the sum of the upper and lower coal seams); Type B, close distance thick coal seam group (the comprehensive mining thickness of the upper and lower coal seams is less than the sum, the mining influence among coal seams is small). This paper focuses on the selection of mining technology for Type A ultra-thick coal seam.

4. Change Characteristic of Support Load in Ultra-thick Coal Seam Multi-layer Mining

Based on evolution process of roof bearing structure in ultra-thick coal seam multi-layer mining, the support load and its change characteristic under different roof bearing structures are analyzed theoretically.

4.1. Evolution Process of Roof Bearing Structure in Multi-Layer Mining of Ultra-Thick Coal Seam

The physical model is constructed for analyzing the evolution process of roof bearing structure in ultra-thick coal seam multi-layer mining, based on the occurrence conditions of group B coal at Dajingnan No. 1 coal mine. The stratigraphy information and model is shown in Figure 11.

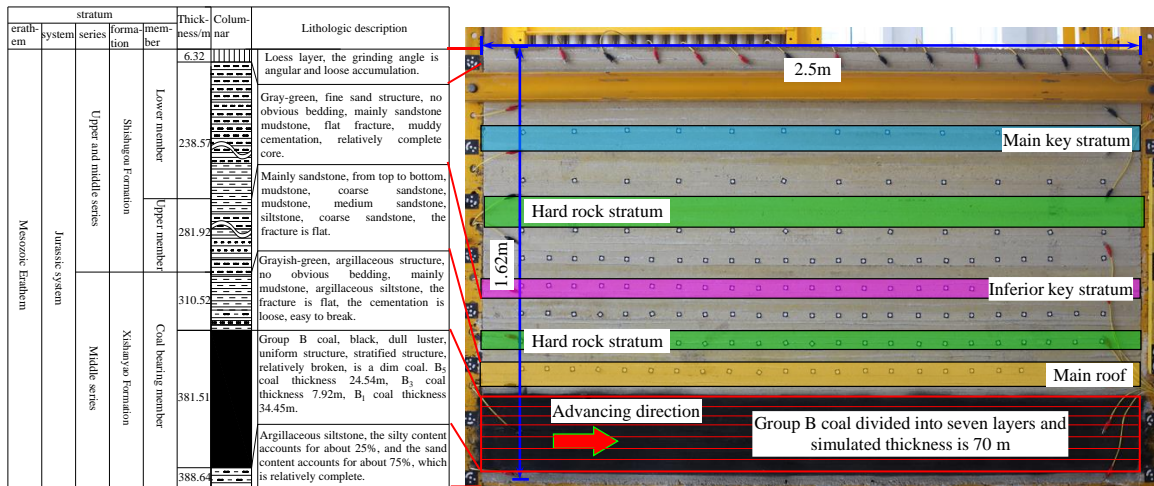


Figure 11. Stratigraphy information and physical model.

It has dimensions of 2.5 m (length) by 0.2 m (width) by 1.62 m (height), with the geometric ratio of 1:240 (model to in situ). The length of the simulated coal seam is 415 m and the overburden thickness is 310 m. There are 92.5 m boundary pillars at both ends of the model to minimize the boundary effects. The overburden lithology is dominated by fine sandstone and mudstone. The uniaxial compressive strength of fine sandstone is 17.46 MPa, the cohesive force is 1.81 MPa, and the uniaxial compressive strength of mudstone is 14.21 MPa, and the cohesive force is 1.41 MPa. With reference to the current mining methods in the area, ultra-thick coal seam is mined in seven layers with a thickness of 10 m.

In the process of multi-layer mining, the roof bearing structure shows the evolution process of “beam structure–higher beam structure–arch structure”, as shown in Figure 12 [22]. With the increase of total coal seam mining thickness, roof bearing structure keeps moving upward, and the height of caving zone increases. The support load changes due to the range increase of instability strata.

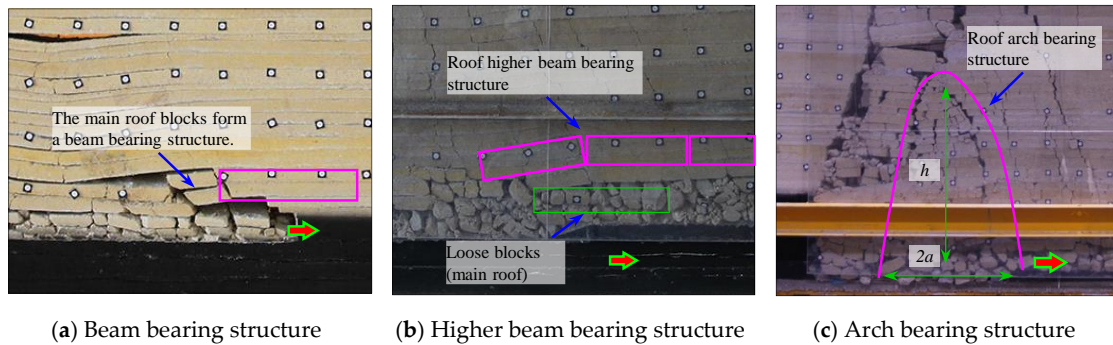


Figure 12. Evolution process of roof bearing structure in multi-layer mining.

4.2. Change Characteristic of the Load on Support under Different Roof Bearing Structures

4.2.1. Support Load under Roof Beam Bearing Structure

At the early stage of multi-layer mining, collapse rock blocks can effectively support the overlying strata, and broken main roof blocks form a beam bearing structure. The support load is mainly the gravity load of immediate roof and top coal and the load caused by rotary subsidence of the main roof blocks, as shown in Figure 13. Considering that top coal and immediate roof are thick and the breakage length of main roof is big, the support load can be known from Equation (1) [23].

$$P = \sum h_i \gamma_i l_m + \left[1 - \frac{L \tan(\varphi - \theta)}{2(H - \Delta)} \right] Q \tag{1}$$

where P is the support load; h_i and γ_i are the thickness and volume force of the i -th stratum (top coal) under the main roof, respectively; l_m is the roof control distance; L is the periodic breakage length of the main roof. As well, θ is the main roof fracture angle; φ is the internal friction angle of the main roof; H is the main roof thickness; Δ is the subsidence of the main roof; Q is the weight of the broken main roof blocks and the load on the blocks.

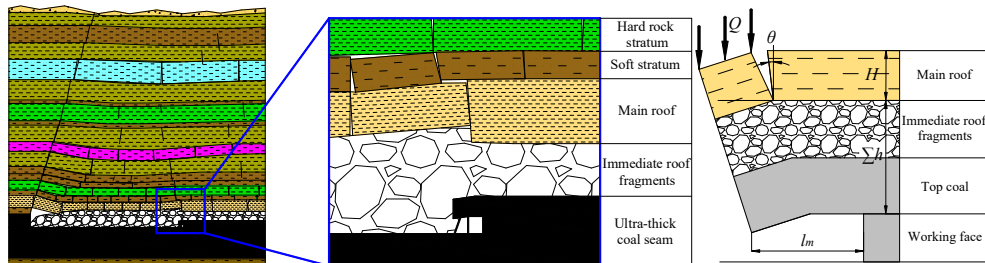
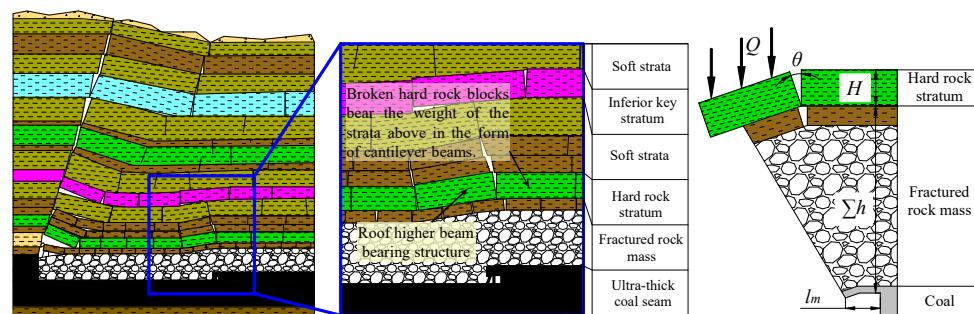


Figure 13. Relationship between support and surrounding rock under roof beam bearing structure.

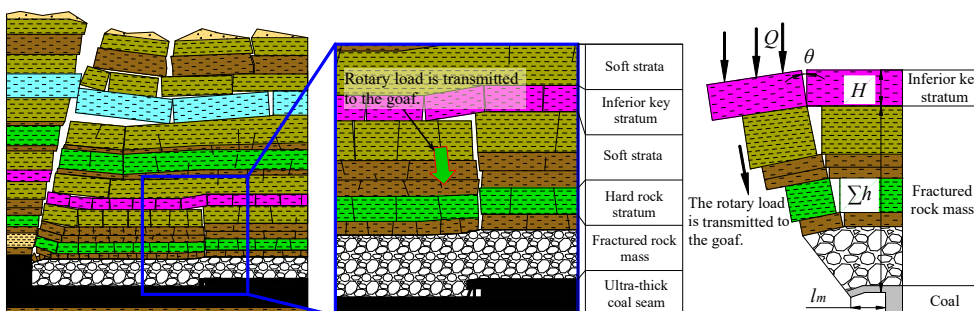
4.2.2. Support Load under Roof Higher Beam Bearing Structure

At the middle stage of multi-layer mining, the hinge of broken main roof blocks weakens, and broken blocks of the higher hard rock stratum hinge to form a higher beam bearing structure. At this time, although the hard rock stratum above the working face has been broken at early stage of mining, the broken hard rock blocks can still bear the weight of the upper rock strata in the form of cantilever beam, because of small suspension length and high strength.

The load on support is mainly resulted from the weight of blocks under the hard rock stratum and the rotation of the broken rock blocks in the hard rock stratum, as shown in Figure 14a. The force condition of roof is similar to that under roof beam bearing structure, and the load on support can be obtained from Equation (1). The corresponding main roof parameters are replaced by those of the hard rock stratum forming the higher beam bearing structure.



(a) Hard rock stratum is close to stope



(b) Hard rock stratum is far from stope

Figure 14. Relationship between support and surrounding rock under roof higher beam bearing structure.

If the roof higher beam bearing structure is far away from the stope, the load generated by the rotary subsidence of the broken hard rock block is transmitted to the goaf, as shown in Figure 14b. The load on support is the gravity load of rock blocks under the hard rock stratum and can be obtained from Equation (2).

$$P = \sum h_i \gamma_i l_m \tag{2}$$

4.2.3. Support Load under Roof Arch Bearing Structure

At the later stage of mining, with the increase of mined volume of rock mass, the hinged structure within the hard rock stratum fails, leading to the roof higher beam bearing structure instability. As well, roof bearing structure is gradually moved upward, the upper rock blocks are compressed together to form an arch bearing structure. The support load is mainly from the gravity load of loose blocks in the arch, as shown in Figure 15.

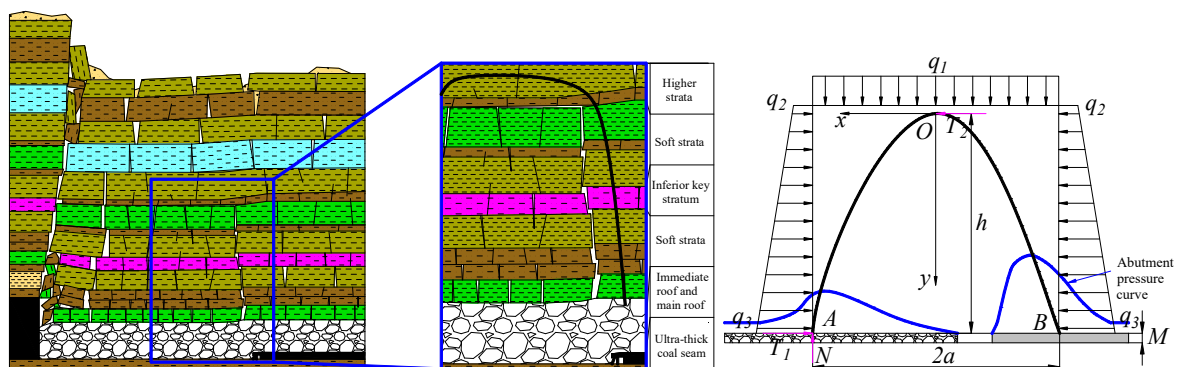


Figure 15. Relationship between support and surrounding rock under roof arch bearing structure.

The essence of roof arch bearing structure is pressure arch AOB, which formed by the mutual extrusion of overburden broken rock blocks. As well, the arch foot is at peak of abutment pressure in the goaf and coal body in front of working face. Pressure arch can withstand compressive stress but cannot withstand bending stress. The loads acting on the pressure arch include weight of rock strata above the arch bearing structure (q_1) and lateral pressure (q_2 and q_3). Taking the AO section for analysis, the vault O is affected by the horizontal force T_2 , and the arch foot A affected by the horizontal force T_1 and the supporting force N . The balance condition of pressure arch is that bending moment and the shear force are 0 at any point on the arch line AOB. According to the balance condition of the model, Equations (3) and (4) can be obtained, and $2a$ is pressure arch span.

$$T_2 h - \frac{1}{2} q_1 a^2 - \int_0^h \left(q_2 + \frac{q_3 - q_2}{h} y \right) dy = 0 \tag{3}$$

$$T_2 = T_1 + \int_0^h \left(q_2 + \frac{q_3 - q_2}{h} \right) dy = 0 \tag{4}$$

$$T_1 = N f = q_1 a f \tag{5}$$

It can be obtained according to Equations (3)–(5).

$$\left(\frac{2}{3} q_2 + \frac{1}{3} q_3 \right) h^2 + 2 a q_1 f h - q_1 a^2 = 0$$

$$h = \frac{q_1 a}{q_1 f + \sqrt{q_1^2 f^2 + q_1 \left(\frac{2}{3} q_2 + \frac{1}{3} q_3 \right)}} \tag{6}$$

where f is static friction coefficient of the surrounding rock, $f = \tan\varphi$, and φ is internal friction angle of surrounding rock in the goaf.

If $q_2 = q_3 = \lambda q_1$, Equation (7) can be obtained.

$$h = \frac{a}{f + \sqrt{f^2 + \lambda}} \quad (7)$$

With the advance of the working face, the arch span increases. When the pressure arch becomes unstable, the roof pressure is the maximum gravity load of the loose blocks in the arch, as shown in Equation (8).

$$P = \sum h_{1i} \gamma_{1i} l_m \quad (8)$$

where h_{1i} and γ_{1i} are the thickness and volume force of the i -th loose body layer below the roof arch bearing structure, respectively.

4.2.4. Support Load Change Characteristic under Different Roof Bearing Structures

The above analysis makes clear calculation method of the support load under different roof bearing structures. When it is roof beam bearing structure, roof pressure usually reaches the maximum value during the first layer mining. When under other roof bearing structure, it is necessary to determine the position of hard rock stratum that can form stable bearing structure firstly, and then determine the form of roof bearing structure by comparing with pressure arch height, the support load value can be obtained finally.

a. Discrimination of Roof Bearing Structure Form

In the rest of the layers mining, rotation angle of broken hard rock blocks can be obtained from Equation (9).

$$\sin\beta = \frac{1}{l} [M - H_1(K_{p'} - 1) - H_2(K_{p''} - 1)] = \frac{1}{l} [M - H_3(K_p - 1)] \quad (9)$$

where β is rotation angle of broken hard rock blocks; M is the thickness of mining layer of coal seam; H_1 and $K_{p'}$ are thickness and residual expansion of caving zone under the roof bearing structure, respectively. H_2 and $K_{p''}$ are thickness and residual expansion of fissure zone under the roof bearing structure, respectively. As well, H_3 and K_p are thickness and residual expansion of rock strata under the roof bearing structure, respectively. l is periodic breakage length of hard stratum.

Equation (10) can be obtained from Equation (9).

$$\frac{H_3}{M} = \left(1 - \frac{l}{M} \sin\beta\right) / (K_p - 1) \quad (10)$$

In Dajingnan No.1 coal mine, the slicing mining thickness is 10 m and periodic breakage length of the hard stratum is 25–30 m. When K_p is 1.1 and maximum rotation angle of broken hard rock blocks is 5–8°, it can be obtained as follow.

$$\frac{H_3}{M} = (1 - 3 \sin\beta) / (1.1 - 1) = 5.82 \sim 7.39 \quad (11)$$

$$H_3 = (5.82 \sim 7.39)M \quad (12)$$

Therefore, when there is a hard rock stratum at H_3 above the roof and $H_3 <$ pressure arch height h , the roof bearing structure is a higher beam bearing structure, and the thickness of rock strata between the roof bearing structure and stope is H_3 . When there are hard rock strata at H_3 above the roof and $H_3 >$ pressure arch height h , the roof bearing structure is an arch bearing structure. In other cases, the height of roof bearing structure is less than H_3 .

b. Support Load under Different Roof Bearing Structure

The slicing mining thickness of group B coal is 10 m in Dajingnan No.1 coal mine. The evolution process of roof bearing structure and the loading condition of the support under different roof bearing structures are shown in Figure 16.

In the first and second layers mining process, the form of roof bearing structure is beam bearing structure, and the load on support is the largest during the first layer mining. In the first layer mining process, as shown in the Figure 13a, the length and thickness of the broken main roof blocks are 27.96 m and 20 m respectively, and roof control distance is 7 m, according to engineering and geological conditions. The main roof block is subjected to gravity load of the strata under the inferior key stratum. So the maximum support load (P_1) is 10463.37 kN in the first layer mining.

$$P_1 = \sum h_i \gamma_i l_m + \left[1 - \frac{L \tan(\varphi - \theta)}{2(H - \Delta)} \right] Q = (9.8 \times 25 + 5 \times 17) \times 7 + \left[1 - \frac{27.96 \times \tan 30^\circ}{2 \times (20 - 6.08)} \right] (27.96 \times 28 \times 25) = 10463.37 \text{ kN} \quad (13)$$

In the third and fourth layers mining process, the roof bearing structure is higher beam structure. During the third layer mining, as shown in the Figure 13b, the main roof blocks collapse, and the broken hard rock blocks 37.8 m away from the stope hinge to form a roof higher beam bearing structure, and the length and thickness of the blocks are 30.53 m and 14.7 m respectively. The block of hard rock stratum is subjected to gravity load of the strata under the inferior key stratum, and the support load (P_2) is 12549.25 kN.

$$P_2 = \sum h_i \gamma_i l_m + \left[1 - \frac{L \tan(\varphi - \theta)}{2(H - \Delta)} \right] Q = (37.8 \times 25 + 5 \times 15) \times 7 + \left[1 - \frac{30.53 \times \tan 30^\circ}{2 \times (14.7 - 3.68)} \right] (30.53 \times 35.4 \times 25) = 12549.25 \text{ kN} \quad (14)$$

In the fourth layer mining, the broken rock blocks in inferior key stratum form a roof higher beam bearing structure, as shown in Figure 13c. Since the roof bearing structure is far from the stope, the support load (P_3) is gravity load of the strata under the inferior key stratum, which is 13160 kN. Compared roof pressure with that under the roof beam bearing structure, the variation range is 25.77%.

$$P_3 = \sum h_i \gamma_i l_m = (72.2 \times 25 + 5 \times 15) \times 7 = 13160 \text{ kN} \quad (15)$$

In the fifth and the rest of the layers mining, roof bearing structure is arch structure. Based on the simulation results [21], the pressure arch span is 210 m, and the pressure arch height is 144.2 m according to Equation (7) (Figure 13d). The maximum support load (P_4) is 25760 kN, and the maximum of support load increases by 146.19% compared with the value under the roof beam bearing structure.

$$P_4 = \sum h_i \gamma_i l_m = (144.2 \times 25 + 5 \times 15) \times 7 = 25760 \text{ kN} \quad (16)$$

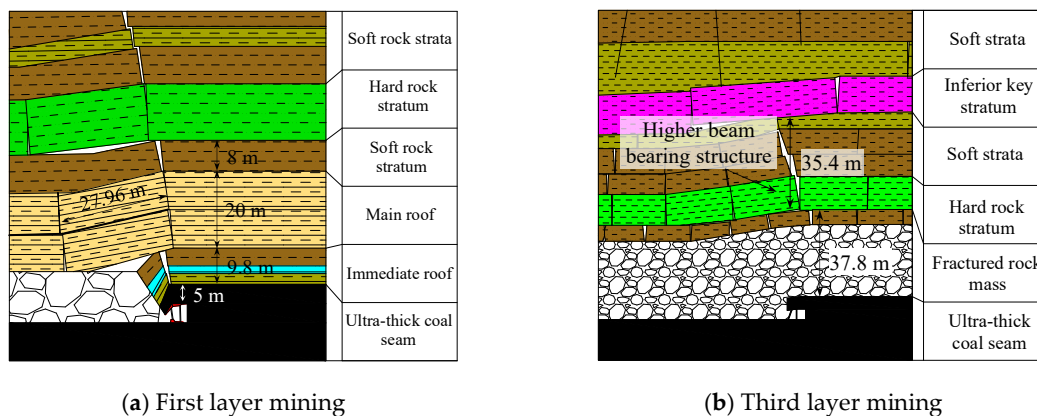


Figure 16. Cont.

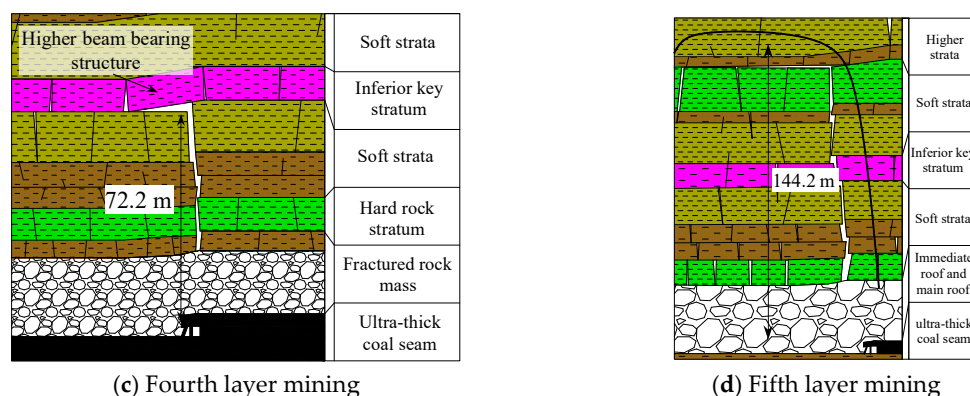


Figure 16. Loading condition of the support under different roof bearing structures.

At the early stage of multi-layer mining, the form of roof bearing structure is beam or higher beam bearing structure, and the maximum support load is around 13,000 kN. At the later stage of mining, the form is arch bearing structure, the support load is close to 26,000 kN, and the current equipment is difficult to meet the needs. The variation of support load is small under beam and higher beam structure, while it increases greatly under arch structure.

5. Classification and Mining Technology Selection of Ultra-thick Coal Seam

In order to realize safe mining of ultra-thick coal seam, this paper analyzes the height development characteristic of the roof bearing structure in multi-layer mining under different occurrence conditions, and classifies the ultra-thick coal seam with the occurrence conditions as the index. The suitable mining technologies are put forward.

5.1. Height Development Characteristics of Roof Bearing Structure in Multi-layer Mining

The dip angle of ultra-thick coal seam is between 0° and 54° , and there are differences in strata failure process under different dip angles in multi-layer mining. Based on the conditions of the group B coal at the Dajingnan No. 1 coal mine, GPU Continuum-based Discrete Element Method software (GDEM, GDEM Technology, Beijing, Co., Ltd., Beijing, China) was used to conduct numerical simulation analysis on the height development process of the roof bearing structure under different coal seam dip angles.

The model size is 700 m (length) by 382 m (height), and the vertical direction is from the coal floor to the surface. The boundary conditions are shown in Table 1, where the side and bottom boundary displacement are constrained, and the upper boundary is representing the free surface. The total thickness of the coal seam is 70 m, divided into seven mining layers. A total of 500 m of each multi-layer is extracted, and there are 100 m wide barrier pillar left to minimize the boundary effects. The dip angles of coal seam are selected as 0° , 10° , 20° , 30° and 45° , respectively. The simulation scheme is shown in Table 1.

Table 1. Simulating scheme of roof bearing structure height development characteristics under different dip angles.

| Model size | Simulating scheme | | |
|------------|------------------------|-------------------------|-------------------------|
| | Coal seam dip angle 0° | Coal seam dip angle 10° | Coal seam dip angle 20° |
| | | | |

In the process of multi-layer mining of inclined ultra-thick coal seam, as shown in Figure 17, roof bearing structure shows the evolution process of “beam structure–higher beam structure–arch structure”, which is consistent with the multi-layer mining of horizontal ultra-thick coal seam.

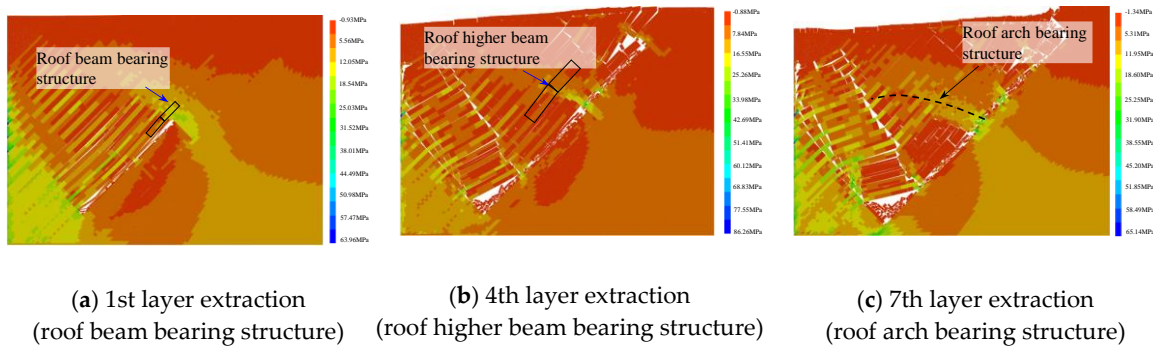


Figure 17. Evolution process of roof bearing structure of inclined ultra-thick coal seam (coal seam dip angle 45°).

The position of roof bearing structure is determined by the peak position of the maximum principal stress. The change curve of roof bearing structure development height is shown in Figure 18.

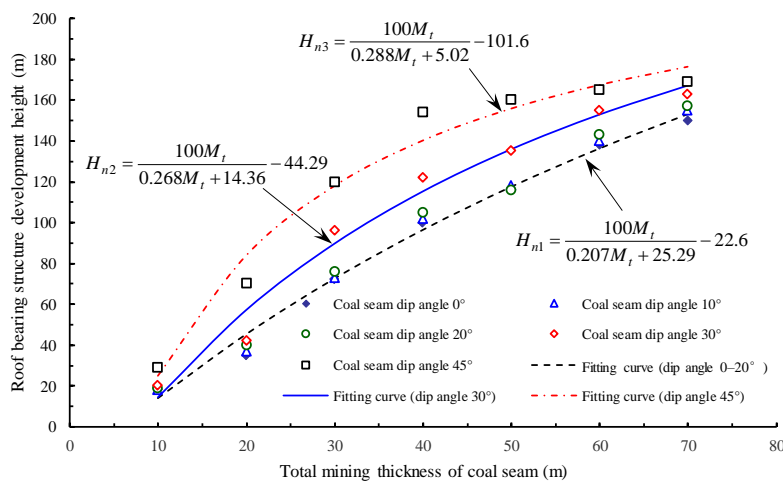


Figure 18. Change curve of the roof bearing structure development height under different dip angle coal seam.

As increase of the total mining thickness of coal seam (M_t), the roof bearing structure gradually moves up and stabilizes at 150 m (pressure arch height h) above the coal seam. Moreover, with increase of coal seam dip angle, the sensitivity of roof bearing structure increases, the stability weakens and the development speed is faster. If dip angle of coal seam is less than 20° , the roof bearing structure is relatively stable, and height of roof bearing structure develops to around 150 m above the coal seam at a total mining thickness of 70 m. If dip angle of coal seam is more than 20° , the roof bearing structure is more sensitive. When the dip angle of coal seam is 30° and 45° , the height of roof bearing structure develops to 150 m at a total mining thickness of 60 m and 40 m, respectively.

The support load is different under different roof bearing structures. In order to classify ultra-thick coal seams, roof bearing structure form is taken as the classification basis, and overlying strata thickness (H_M), roof bearing structure height (H_n) and pressure arch height (h) are taken as the classification indexes. The ultra-thick coal seams classified as shown in Table 2.

Table 2. Classification of ultra-thick seams.

| Types | Classification conditions | Roof bearing structure form | Development height of roof bearing structure (H_n) |
|--------------------|----------------------------|---------------------------------|---|
| Type I coal seam | $H_M < H_n$ | no stable bearing structure | Dip angle of coal seam $\alpha \leq 20^\circ$; $H_{n1} = 100M_t/(0.207M_t + 25.29) - 22.6$ |
| Type II coal seam | $H_n < h$ and $H_n < H_M$ | (higher) beam bearing structure | $20^\circ < \text{dip angle of coal seam } \alpha < 30^\circ$; $H_{n2} = 100M_t/(0.268M_t + 14.36) - 44.29$ |
| Type III coal seam | $H_n \geq h$ and $h < H_M$ | arch bearing structure | $30^\circ \leq \text{dip angle of coal seam } \alpha$; $H_{n3} = 100M_t/(0.288M_t + 5.02) - 101.6$ |

According to the form of roof bearing structure, ultra-thick coal seams can be divided into three types:

- If $H_M < H_n$, ultra-thick coal seam belongs to type I coal seam. There is no stable bearing structure in the roof strata, and the support load at the later stage of mining is all or most of gravity load of overburden strata.
- If $H_n < h$ and $H_n < H_M$, ultra-thick coal seam belongs to type II coal seam. The roof bearing structure is (higher) beam structure, and the support load is the gravity load of rock strata under the bearing structure and the load caused by the rotary subsidence of broken hard rock blocks.
- If $H_n \geq h$ and $h < H_M$, ultra-thick coal seam belongs to type III coal seam. At the later stage of mining, the roof bearing structure is arch structure, and the load on support is mainly the gravity load of loose blocks under the arch.

5.2. Mining Technology Selection of Ultra-thick Coal Seam

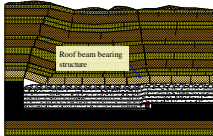
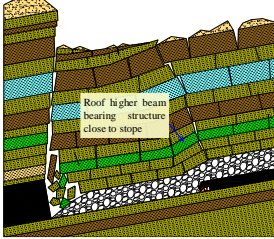
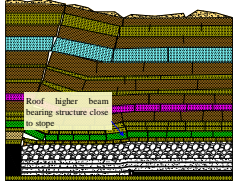
At the later stage of the multi-layer mining, the roof bearing structure evolves into arch bearing structure, and the load on support rises from 13,000 kN to 26,000 kN, and the current equipment is difficult to meet. In order to reduce the stope roof pressure, suitable mining technology should be selected to control the form and height of the roof bearing structure and reduce the range of rock strata that transmits gravity load.

From the above analysis, it can be seen that the artificial controllable factor of the roof bearing structure form is the slicing mining thickness in multi-layer mining of ultra-thick coal seam. The smaller slicing mining thickness of coal seam is, the smaller rotation angle of broken rock block in hard stratum is, and the more stable the (higher) beam bearing structure is. However, as the number of slicing mining layers increases, on the one hand, thick and hard rock strata separate easily along the weak structural plane, resulting in blocks secondary breakage, which reduces the stability of the bearing structure. On the other hand, production costs increase. On the premise that the slicing mining thickness can meet the production demand, shortwall mining and backfill mining should be adopted to reduce equivalent mining thickness of the coal seam, limit the movement space of roof strata, and control the roof bearing structure form and development height. Therefore, the mining technology selection for ultra-thick coal seam should be based on the principle of “ensuring the stability of near-stope roof

bearing structure”, so as to avoid the appearance of the roof arch bearing structure and reduce the height of higher beam bearing structure.

Combined with the occurrence conditions, mining technology and classification standards, the underground mining technology of ultra-thick coal seam with average thickness of more than 20 m is studied. The main contents are shown in Table 3.

Table 3. Selection of mining technology for typical ultra-thick coal seams in Xinjiang.

| Types | Type I coal seam | Type II coal seam | Type III coal seam |
|---|--|--|---|
| Typical mining areas and coalfields | / | <p>Ili Coalfield: The average thickness of 5# coal in Yining mining area is 21.36 m. The thickness of C₁-C₅ group coal in Nilka mining area is 26 m.</p> <p>Turpan-Harmi Coalfield: The thickness of 13 # coal in Toksun Heishan mining area is 32.09 m.</p> <p>East Junggar Coalfield: The average thickness of B₂ coal in Jiangjunmiao mining area is 30.62 m.</p> | <p>Turpan-Harmi Coalfield: The average thickness of C₈ coal in Shaerhu coalfield is 96.82 m.</p> <p>East Junggar Coalfield: The average thickness of B coal in Dajing mining area is 70 m.</p> |
| Mining technology | Backfill mining | Longwall caving mining is adopted in seams with small dip angle or thickness of 20–30 m, and backfill mining is adopted in seams with large dip angle. | Longwall mining at the early stage, backfill mining at the later stage. |
| Schematic diagram of the roof bearing structure control |  |  <p>When longwall caving mining, near-stope higher beam bearing structure can keep stable</p> |  |
| | <p>Backfill mining limits the movement space of roof strata and ensures the stability of beam bearing structure.</p> | <p>When the dip angle of coal seam is large, backfill mining is adopted to ensure the stability of beam bearing structure (near-stope higher beam bearing structure).</p> | <p>Longwall mining at the early stage, backfill mining at the later stage, beam bearing structure instability, near-stope higher beam bearing structure keeps stable</p> |

a. Type I ultra-thick coal seam that is not suitable for open pit mining

There is no stable bearing structure in the roof strata, and the load on support at the later stage of mining is from gravity load of rock strata under the bearing structure of the rock mass. Therefore, in order to reduce support load, backfill mining is adopted to reduce equivalent mining thickness, improve the stability of beam bearing structure, and control the development of caving zone.

b. Type II ultra-thick coal seam

For ultra-thick coal seam with small dip angle, height of the roof bearing structure is developed slowly, and the near-stope roof higher beam structure is more stable, so longwall mining can be adopted. For ultra-thick coal seam with large dip angle, the roof bearing structure is sensitive. At the later stage of mining, it is easy to form the far-stope higher beam structure. As well, the support load is easy to suddenly increase with the instability of the roof higher beam bearing structure, backfill mining is a better choice. If the coal thickness is around 20 m, the roof bearing structure has a small development height, ultra-thick seam can be mined by longwall mining.

c. Type III ultra-thick coal seam

The backfill mining should be adopted to reduce equivalent mining thickness so as to avoid the roof arch bearing structure. On the premise of ensuring reasonable development height of the roof bearing structure, longwall mining can be adopted at the early stage and backfill mining at the later stage. If total mining thickness is large, the hydraulic support is subjected to a large gravity load of the backfilled body when the slicing backfill mining is adopted, and the remaining part of the coal seam should not be mined.

6. Conclusions and Prospects

Based on coal resource exploration in Xinjiang, this paper analyzed the occurrence characteristic of ultra-thick coal seams in Xinjiang. The change characteristic of support load under different roof bearing structures in multi-layer mining of ultra-thick coal seam was studied. From the perspective of coal mining, classification and mining technology selection of ultra-thick coal seams were put forward.

The ultra-thick coal seams in Xinjiang have a distribution characteristic of more north and less south, more east and less west, mainly concentrate in East Junggar and Turpan-Harimi coalfields. The C₈ coal seam of Shaerhu coal field and the group B coal seams of East Junggar coal field are the most representative ultra-thick coal seams, with coal seam thickness of 96.82 m and 70–90 m respectively, and the maximum thickness of C₈ coal seam in the Shaerhu coalfield is 267.42m. The buried depth of the coal seam is between 300 m and 600 m, and the dip angle, number of layers and thickness of the coal seam change greatly. The form of the ultra-thick coal seam has the remarkable characteristic of coal seams merging and bifurcating.

Based on the evolution process of the roof bearing structure during ultra-thick coal seam multi-layer mining, the mechanical model of the relationship between the support and surrounding was established, considering different roof bearing structures. As well, the change characteristic of support load in multi-layer mining of a typical ultra-thick coal seam in Xinjiang is studied. In the process of multi-layer mining, the roof bearing structure shows the evolution process of “beam structure-higher beam structure-arch structure”. At the early stage of multi-layer mining, the load on support is rotary subsidence load of the near-stope roof bearing structure and gravity load of rock strata under the bearing structure. At the later stage, the support load is mainly gravity load of loose blocks under the far-stope bearing structure. The change of support load is small under beam and higher beam bearing structures, while it increases greatly under arch bearing structure.

Based on the form and development height of the roof bearing structure under different occurrence conditions, classification method and mining technology selection of ultra-thick coal seam are put forward. Overlying strata thickness (H_M), roof bearing structure height (H_n) and pressure arch height (h) are taken as the ultra-thick classification indexes, and the mining technology selection principle of “ensuring the stability of the near-stope roof bearing structure” is proposed. Ultra-thick coal seam divides into three types: No stable bearing structure, (higher) beam bearing structure and arch bearing structure. In order to ensure the stability of the near-stope roof bearing structure, three types of ultra-thick coal seams should be mined by using backfill mining, longwall mining and early longwall mining, later backfill mining, respectively.

The occurrence conditions of ultra-thick coal seams in Xinjiang are complex and variable, the degree of exploration is low, and the surface ecological environment is also fragile. Large-scale mining of ultra-thick coal seams has just begun, a series of problems need to be studied systematically. In this paper, the distribution and occurrence characteristics of ultra-thick coal seams are studied. Based on the change characteristics of roof bearing structure and support load, classification of ultra-thick coal seams is proposed, and suggestion on the selection of mining technology is put forward.

In the actual mining process, it is necessary to balance relationship between the hydraulic support performance and coal recovery rate by flexibly selecting mining technology. Mining technological parameters, coal seam slicing thickness determination and measures of roof control technology are still the research focus in the field of ultra-thick coal seams reasonable and efficient mining.

Author Contributions: Writing—original draft preparation, D.Q.; data processing, X.W. and D.Z.; writing—review and editing, W.G.; partially participation in the literature research, L.Z. and M.X.

Funding: This research was funded by the National Natural Science Foundation of China, grant number 51474206 and 51404254; National Key Basic Research Program of China, grant number 973 Program- No.2015CB251600 and the Project Funded by the Priority Academic Program Development of Jiangsu Higher Education Institutions (PAPD).

Acknowledgments: The authors would like to thank the editor and the reviewers for their contributions on the paper.

Conflicts of Interest: The authors declare no conflict of interest.

References

1. Volkov, V.N. Phenomenon of the Formation of Very Thick Coal Beds. *Lithol. Miner. Resour.* **2003**, *38*, 223–232. [[CrossRef](#)]
2. Wang, D.D.; Shao, L.Y.; Liu, H.Y.; Shao, K.; Yu, D.M.; Liu, B.Q. Research progress in formation mechanisms of super-thick coal seam. *J. China Coal Society* **2016**, *41*, 1487–1497.
3. Rošer, J.; Potočnik, D.; Vulić, M. Analysis of Dynamic Surface Subsidence at the Underground Coal Mining Site in Velenje, Slovenia through Modified Sigmoidal Function. *Minerals* **2018**, *8*, 74. [[CrossRef](#)]
4. Khan, I.; Javed, A. Spatio-Temporal Land Cover Dynamics in Open Cast Coal Mine Area of Singrauli, M.P., India. *J. Geogr. Inf. Syst.* **2012**, *4*, 521–529. [[CrossRef](#)]
5. Zarlín, N.; Sasaoka, T.; Shimada, H.; Matsui, K. Numerical Study on an Applicable Underground Mining Method for Soft Extra-Thick Coal Seams in Thailand. *Engineering* **2012**, *4*, 739–745. [[CrossRef](#)]
6. Lin, N.; Sasaoka, T.; Shimada, H.; Hamanaka, A.; Matsui, K. Numerical Analysis of Interaction Effects in Double Extra-thick Coal Seams Mining. *Procedia Earth Planet. Sci.* **2013**, *6*, 343–349. [[CrossRef](#)]
7. Islam, M.R.; Hayashi, D.; Kamruzzaman, A. Finite element modeling of stress distributions and problems for multi-slice longwall mining in Bangladesh, with special reference to the Barapukuria coal mine. *Int. J. Coal Geol.* **2009**, *78*, 91–109. [[CrossRef](#)]
8. Hu, S.R.; Lin, L.N.; Huang, C.; Chen, D.Y.; Hao, G.Q. Distribution and genetic model of extra-thick coal seams. *Coal Geol. China* **2011**, *23*, 1–5.
9. Shearer, J.C.; Staub, J.R.; Moore, T.A. The Conundrum of Coal Bed Thickness: A Theory for Stacked Mire Sequences. *J. Geol.* **1994**, *102*, 611–617. [[CrossRef](#)]
10. Large, D.J.; Marshall, C. Use of carbon accumulation rates to estimate the duration of coal seams and the influence of atmospheric dust deposition on coal composition. In *Strata and Time: Probing the Gaps in Our Understanding*; Geological Society: London, UK, Special Publications, 2014. [[CrossRef](#)]
11. Nadon, G.C. Magnitude and timing of peat-to-coal compaction. *Geology* **1998**, *26*, 727. [[CrossRef](#)]
12. Diessel, C.; Boyd, R.; Wadsworth, J.; Leckie, D.; Chalmers, G. On balanced and unbalanced accommodation/peat accumulation ratios in the Cretaceous coals from Gates Formation, Western Canada, and their sequence-stratigraphic significance. *Int. J. Coal Geol.* **2000**, *43*, 143–186. [[CrossRef](#)]
13. Diessel, C.F. Utility of coal petrology for sequence-stratigraphic analysis. *Int. J. Coal Geol.* **2007**, *70*, 3–34. [[CrossRef](#)]
14. Wu, C.; Li, S.; Wang, G.; Liu, G.; Kong, C. The allochthonous genesis model about the extra-thick and high-quality coalbed in Xianfeng basin, Yunnan Province, China. *Front. Earth Sci. China* **2007**, *1*, 97–105. [[CrossRef](#)]
15. Holz, M.; Kalkreuth, W.; Banerjee, I. Sequence stratigraphy of paralic coal-bearing strata: An overview. *Int. J. Coal Geol.* **2002**, *48*, 147–179. [[CrossRef](#)]
16. Jerrett, R.M.; Davies, R.C.; Hodgson, D.M.; Flint, S.S.; Chiverrell, R.; Chiverrell, R. The significance of hiatal surfaces in coal seams. *J. Geol. Soc.* **2011**, *168*, 629–632. [[CrossRef](#)]
17. Li, Z.X.; Wang, D.D.; Lv, D.W.; Li, Y.; Liu, H.Y.; Wang, P.L.; Liu, Y.; Liu, J.Q.; Li, D.D. The geologic settings of Chinese coal deposits. *Int. Geol. Rev.* **2018**, *60*, 548–578. [[CrossRef](#)]
18. Zhang, D.S.; Liu, H.L.; Fan, G.W.; Wang, X.F. Connotation and prospection on scientific mining of large Xinjiang coal base. *IJMME* **2015**, *32*, 1–6.
19. Li, Y.H.; Zhao, F.H.; Nie, H.G. *Jurassic coal accumulation law of main coal-bearing basins in Eastern Xinjiang*; Science Press: Beijing, China, 2015.

20. Li, J.; Zhuang, X.G.; Querol, X.; Font, O.; Moreno, N.; Zhou, J.B.; Lei, G.M. High quality of Jurassic coals in the Southern and Eastern Junggar Coalfields, Xinjiang, NW China: Geochemical and mineralogical characteristics. *Int. J. Coal Geol.* **2012**, *99*, 1–15. [[CrossRef](#)]
21. Zhou, J.; Zhuang, X.; Alastuey, A.; Querol, X.; Li, J. Geochemistry and mineralogy of coal in the recently explored Zhundong large coal field in the Junggar basin, Xinjiang province, China. *Int. J. Coal Geol.* **2010**, *82*, 51–67. [[CrossRef](#)]
22. Wang, X.F.; Qin, D.D.; Zhang, D.S.; Guan, W.M.; Xu, M.T.; Wang, X.L.; Zhang, C.G. Evolution characteristics of overburden strata structure for ultra-thick coal seam multi-layer mining in Xinjiang east Junggar basin. *Energies* **2019**, *12*, 332. [[CrossRef](#)]
23. Jin, Z.M. *Theory and Technology of Top Caving Coal Mining*; China Coal Industry Publishing House: Beijing, China, 2001; pp. 1–258.



© 2019 by the authors. Licensee MDPI, Basel, Switzerland. This article is an open access article distributed under the terms and conditions of the Creative Commons Attribution (CC BY) license (<http://creativecommons.org/licenses/by/4.0/>).